Controllable motion of optical vortex arrays using electromagnetically induced transparency

David Shwa,* Evgeny Shtranvasser, Yoni Shalibo, and Nadav Katz

The Racah Institute of Physics, The Hebrew University, Jerusalem 91904, Israel

*david.shwa@mail.huji.ac.il

Abstract: We demonstrate control of the collective motion of an optical vortex array using an electromagnetically induced transparency media. Scanning the frequency detuning between the pump and probe fields changes the susceptibility of the media, producing a unique effective diffraction of the vortex array for each detuning. We measure several experimental configurations and compare them to numerical simulations.

OCIS codes: (020.1670) Coherent optical effects; (050.4865) Optical vortices; (070.4690) Morphological transformations.

References and links

1. K. Boller, A. Imamoglu, and S. Harris, "Observation of electromagnetically induced transparency," Phys. Rev. Lett. **66**, 2593–2596 (1991).
2. M. Fleischhauer, A. Imamoglu, and J. Marangos, "Electromagnetically induced transparency: optics in coherent media," Rev. Mod. Phys. **77**, 633–673 (2005).
3. P. K. Vudyasetu, D. Starling, and J. C. Howell, "All optical waveguiding in a coherent atomic rubidium vapor," Phys. Rev. Lett. **102**, 123602 (2009).
4. O. Firstenberg, P. London, M. Shuker, A. Ron, and N. Davidson, "Elimination, reversal and directional bias of optical diffraction," Nat. Phys. **5**, 665–668 (2009).
5. O. Firstenberg, M. Shuker, N. Davidson, and A. Ron, "Elimination of the diffraction of arbitrary images imprinted on slow light," Phys. Rev. Lett. **102**, 043601 (2009).
6. M. Shuker, O. Firstenberg, R. Pugatch, A. Ron, and N. Davidson, "Storing images in warm atomic vapor," Phys. Rev. Lett. **100**, 223601 (2008).
7. L. Zhao, T. Wang, Y. Xiao, and S. F. Yelin, "Image storage in hot vapors," Phys. Rev. A **77**, 041802 (2008).
8. H. He, M. Friese, N. Heckenberg, and H. Rubinsztein-Dunlop, "Direct observation of transfer of angular momentum to absorptive particles from a laser beam with a phase singularity," Phys. Rev. Lett. **75**, 826–829 (1995).
9. A. Mair, A. Vaziri, G. Weihs, and A. Zeilinger, "Entanglement of the orbital angular momentum states of photons," Nature **412**, 313–316 (2001).
10. S. Franke-Arnold, L. Allen, and M. Padgett, "Advances in optical angular momentum," Laser Photon. Rev. **2**, 299–313 (2008).
11. R. Pugatch, M. Shuker, O. Firstenberg, A. Ron, and N. Davidson, "Topological stability of stored optical vortices," Phys. Rev. Lett. **98**, 203601 (2007).
12. Z. Chen, J. Pu, and D. Zhao, "Tight focusing properties of linearly polarized Gaussian beam with a pair of vortices," Phys. Lett. A **375**, 2958–2963 (2011).
13. D. Neshev, "Motion control of ensembles of ordered optical vortices generated on finite extent background," Opt. Commun. **151**, 413–421 (1998).
14. G. Indebetouw, "Optical vortices and their propagation," J. Mod. Opt. **40**, 73–87 (1993).
15. D. Rozas, Z. S. Sacks, and G. A. Swartzlander, Jr., "Experimental observation of fluidlike motion of optical vortices," Phys. Rev. Lett. **79**, 3399–3402 (1997).
16. D. Rozas, C. T. Law, and G. A. Swartzlander, Jr., "Propagation dynamics of optical vortices," J. Opt. Soc. Am. B **14**, 3054–3065 (1997).
17. X. Gan, J. Zhao, S. Liu, and L. Fang, "Generation and motion control of optical multi-vortex," Chin. Opt. Lett. **7**, 1142–1145 (2009).

#164287 - $15.00 USD Received 12 Mar 2012; revised 22 Apr 2012; accepted 24 Apr 2012; published 16 Oct 2012

18. O. Firstenberg, M. Shuker, R. Pugatch, D. Fredkin, N. Davidson, and A. Ron, "Theory of thermal motion in electromagnetically induced transparency: effects of diffusion, Doppler broadening, and Dicke and Ramsey narrowing," Phys. Rev. A **77**, 043830 (2008).
19. M. Chen and F. S. Roux, "Accelerating the annihilation of an optical vortex dipole in a Gaussian beam." J. Opt. Soc. Am. A **25**, 1279–1286 (2008).
20. O. Firstenberg, P. London, D. Yankelev, R. Pugatch, M. Shuker, and N. Davidson, "Self-similar modes of coherent diffusion," Phys. Rev. Lett. **105**, 183602 (2010).
21. A. Y. Bekshaev, M. S. Soskin, and M. V. Vasnetsov, "Optical vortex symmetry breakdown and decomposition of the orbital angular momentum of light beams," J. Opt. Soc. Am. A **20**, 1635–1643 (2003).
22. P. K. Vudyasetu, R. M. Camacho, and J. C. Howell, "Storage and retrieval of multimode transverse images in hot atomic rubidium vapor," Phys. Rev. Lett. **100**, 123903 (2008).
23. E. E. Mikhailov, I. Novikova, M. D. Havey, and F. A. Narducci, "Magnetic field imaging with atomic Rb vapor," Opt. Lett. **34**, 3529–3531 (2009).

1. Introduction

The optical susceptibility of atomic media due to a weak resonant probe field can be changed dramatically in the presence of a strong pump field. The imaginary part of the susceptibility vanishes, thus leading to a transparency in the otherwise opaque media, while the real part of the susceptibility becomes very steep, resulting a great reduction in the group velocity as compared with the speed of light. This effect is termed electromagnetically induced transparency (EIT) [1, 2]. An extremely rich variety of spatially dependent optical phenomena that is derived from the complex susceptibility of EIT media was demonstrated recently, such as waveguiding [3], frequency dependent diffraction, diffractionless propagation, Negative diffraction and induced deflection [4, 5]. Transmission of phase dependent patterns were also achieved and highlighted as an effective way to reduce diffusion effects in storage processes [6, 7].

Here we report on a different phenomenon related to the complex susceptibility, namely, a controllable collective motion of optical vortex arrays. An optical vortex is an electromagnetic mode with zero intensity in the center and a cylindrical phase $e^{im\phi}$, where ϕ is defined as an angle variable around the vortex core and m is an integer quantizing the orbital angular momentum (OAM) of the vortex. Optical vortices have a wide range of applications such as optical trapping and tweezing [8], quantum entanglement [9, 10] and contrast enhancement in light microscopy [10]. Single vortex beams were used as a probe beam in EIT experiments, and demonstrated higher stability of the vortex against diffusion effects, as opposed to a bagel shaped flat phase beam [11]. The transverse collective motion of optical vortex array patterns as they propagate in free-space was studied extensively [12–14] and was found to depend upon the total OAM of the array (denoted by L), the average distance between the vortices, the vortices' core size and the background profile they are embedded in. In general, vortex arrays with L$\neq$0 were shown to rotate as the beam propagates due to the collective OAM of the beam, while vortex arrays with L=0 do not rotate at all but can contract and annihilate. The movement of each vortex is determined by the phase and intensity gradients of the beam in the vortex core. Thus the movement of each vortex is driven by the phase created by the other vortices in the array, leading to a collective motion [15–17]. We control this collective motion of the vortex array in EIT media by changing the frequency of our pump field, varying it from resonance with the two-photon transition of the EIT (two-photon detuning).

The concept behind the manipulation of vortex arrays is the controllable diffraction of the probe image due to the tunable susceptibility. For an undepleted plane wave pump beam, the susceptibility of a spatially varying probe in EIT can be written as [18]:

$$\chi_{31}(\mathbf{k}_\perp,\omega) = i\frac{g}{c}K(\omega)n_0\left[1+\tilde{L}(\mathbf{k}_\perp,\omega)\right] \tag{1}$$

where $\mathbf{k}_\perp$ is the transverse wavevector of the probe profile, g is the dipole interaction strength,

#164287 - $15.00 USD Received 12 Mar 2012; revised 22 Apr 2012; accepted 24 Apr 2012; published 16 Oct 2012

n_0 is the density of the vapor, $K(\omega)$ is the dimensionless susceptibility in the absence of the pump field and $\tilde{L}$ is the following spatio-temporal spectral function :

$$\tilde{L}(\mathbf{k}_\perp,\omega)=\frac{K(\omega)|\Omega_c|^2}{i(\Delta+\omega)-\Gamma_{hom}-D\mathbf{k}_\perp{}^2} \tag{2}$$

Here Ω_c is the Rabi frequency of the coupling field, Δ is the two photon detuning, Γ_{hom} is the decoherence rate and $D=\frac{v_{th}^2}{\gamma}$ is the Dicke-Doppler diffusion coefficient where γ is the relaxation rate due to collisions with the buffer gas and $v_{th}=\sqrt{\frac{k_BT}{m}}$ is the thermal velocity of the atoms. The dynamics of the probe pattern due to this complex susceptibility is given by $\partial\mathbf{E}/\partial z = i(\chi_{31}-\frac{\lambda|\mathbf{k}_\perp|^2}{4\pi})\mathbf{E}$, where λ is the optical wavelength. This dynamics can be described as a diffusion equation with a complex diffusion constant, meaning that it undergoes a frequency dependent optical diffraction together with a diffusion due to the atomic motion [18]. The diffraction component creates a behavior similar to the vortex array motion in free-space, but with a frequency controlled effective diffraction length. Hence, as the two photon detuning is scanned we expect to see the effects that were described before in free-space, such as a rotation of vortex arrays with L≠0 and a contraction in the case of arrays with L=0. The diffusion component leads to a motion also in the direction of the intensity gradient and not only perpendicular to it. This outcome is unique to the propagation in diffusive media and has no counterpart in free-space propagation.

A major advantage of this method for applications such as optical trapping and optical wrenches is the ability to move vortices without a physical change of the input probe field, which is usually a slow process, but a frequency control which is potentially much faster and more robust.

2. Experimental setup

Our experimental setup is described in Fig. 1. As the EIT medium we use the D1 transition of ^{87}Rb, where the Λ configuration is comprised of the hyperfine levels. We use a distributed feedback laser as our source of 795 nm beam. This beam is separated into pump and probe beams using a beam splitter. Both beams pass through an acousto-optic modulator, the probe for amplitude control and the pump for amplitude and frequency control using a double pass configuration. A hyperfine splitting of 6.8 GHz is created using an electro-optic modulator on the probe beam followed by an etalon used to filter out the unwanted 0 and -1 orders. The EOM is used also to compensate for the frequency mismatch of the probe due to the double pass of the pump. The spatial phase dependence of the beam is created using a liquid crystal spatial light modulator (BNS, 512×512 pixels). Finally, both the pump and the probe beams are combined using a Glan-Taylor polarizer and pass through a 7.5 cm quartz cell heated to $\sim 40^oC$. The cell contains isotopically pure ^{87}Rb and 20 Torr Neon as buffer gas. After the cell, the pump and probe beams are separated using another Glan-Taylor polarizer and the probe beam is measured using a CCD camera (PCO Pixelfly qe) with short exposure times of $5-10\mu s$ in order to avoid distortions due to phase fluctuations. For the results described here we use a probe beam with a power of $5\mu W$ and a pump beam with a power of $150\mu W$ and a waist of 2.5 mm.

3. Results and discussion

Figure 2 shows the phase patterns imprinted on the spatial light modulator for a 2×2 vortex array in two configurations. The vortex array in Fig. 2(a) comprises two vortices having OAM of +1 and two vortices having OAM of -1, so the total OAM of the pattern is L=0, while in Fig. 2(b) all the vorices have OAM of +1, so the total OAM of the pattern is L=4. We chose these

#164287 - $15.00 USD Received 12 Mar 2012; revised 22 Apr 2012; accepted 24 Apr 2012; published 16 Oct 2012

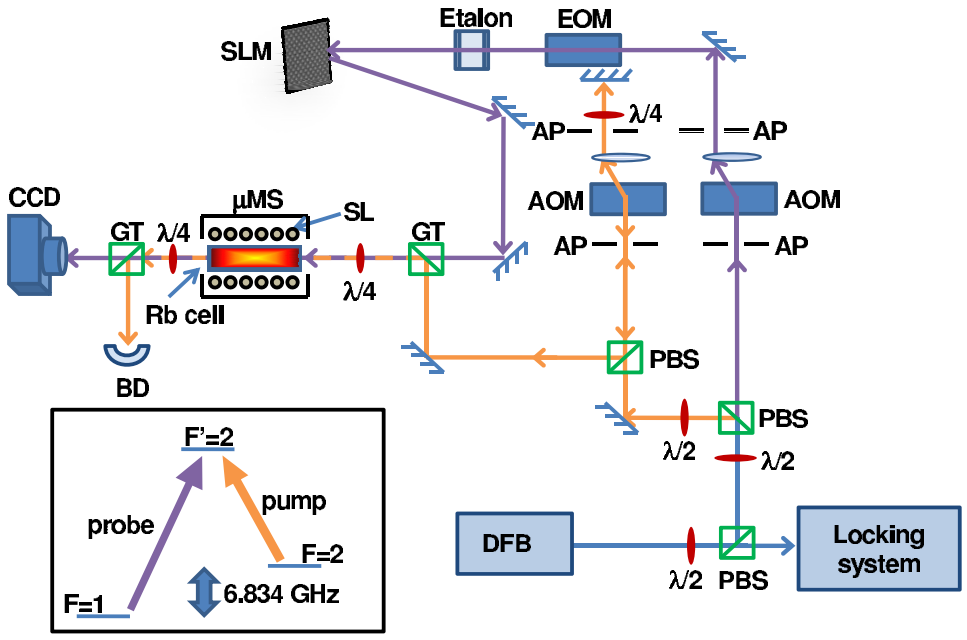

Fig. 1. Our experimental setup. Orange lines - pump beam, purple lines - probe beam. DFB - distributed feedback laser, PBS - polarizing beam splitter, $\lambda/2, \lambda/4$ - waveplates, AP - aperture, GT - Glan-Taylor polarizer, SL - solenoid, SLM - spatial light modulator, AOM - acousto-optic modulator, EOM - electro-optic modulator, BD - beam dump, μMS- μ-metal shield. In the inset - the relevant ^{87}Rb hyperfine level diagram.

two configurations in order to demonstrate the effect of EIT on the two generic possibilities of vortex array, namely, L=0 and L$\neq$0.

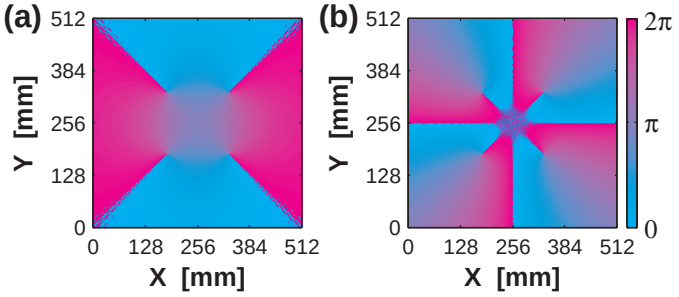

Fig. 2. Phase patterns of a four vortex array. The phase for each point of the pattern is the multiplication of each vortex phase, $\prod_j \exp(im_j\phi_j)$. ϕ_j is defined as $\phi_j = arctan[(y-y_j)/(x-x_j)]$, where (x_j,y_j) is the location of the jth vortex core. Patterns are imprinted on the spatial light modulator with the gaussian probe beam directed to the center of the pattern. (a) Two m=1 and two m=-1 vortices. (b) Four m=1 vortices.

Figures 3(a) and 4(a) present typical results for a vortex array control by changing the two photon detuning using EIT setup. The spatial profile of the probe is a 0.5 mm waist gaussian

#164287 - $15.00 USD Received 12 Mar 2012; revised 22 Apr 2012; accepted 24 Apr 2012; published 16 Oct 2012

beam with a 2×2 vortex array embedded in it. Figure 3(a) is produced using the phase pattern depicted in Fig. 2(a), while Fig. 4(a) is produced using the phase pattern presented in Fig. 2(b).

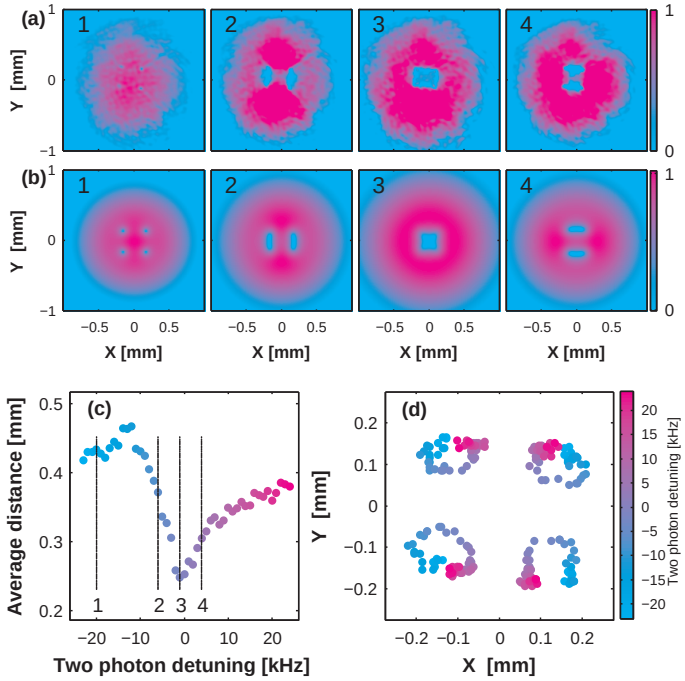

Fig. 3. Experimental results for the collective rotation of four vortices, two m=+1 and two m=-1 with total angular momentum L=0. (a) Pictures for different frequencies with log scaled normalized intensity. The numbers relate to the vertical lines in (c). (b) Pictures of simulations for the same frequencies. (c) The average size of the array measured as the distance between two opposite vortices. The array size at resonance is about half of the original array size. (d) 2D plot of the vortex centers at different detunings. Although each vortex moves in a circular motion as the detuning is scanned, the full array does not rotate but only contracts. Near the resonance (picture (a3)) the four vortices almost combine to one point with zero amplitude and L=0.

Figures 3(b) and 4(b) show simulations based on Eq. (1) of both the situations discussed with good agreement to the experimental results. The simulation uses the measured temperature and pump intensity, while γ is calculated ab initio using a hard sphere model. g and $K(\omega)$ are the only fitting parameters (minor adjustments from calculated/measured values due to experimental uncertainties) used in order to achieve the measured EIT absorption spectrum. Once the EIT spectrum is matched, the spatial propagation is calculated for all patterns without any further fitting.

Figures 3(d) and 4(d) show the dynamics of each vortex center as the two photon detuning is scanned. For L=4 a global rotation accompanied by vortex repulsion is observed (Fig. 4(c)). The rotation is a signature of the non-zero angular momentum of the array while the repulsion has to do with the movement of the vortices due to the gaussian envelope of the beam. This repulsion is higher when the rotation is higher thus leading to a more distorted images for higher total L patterns. The circular trajectory of each vortex as described in Fig. 4(d) is very different from free-space propagation where a linear trajectory was observed [14, 15]. The circular trajectory is due to the combined effects of diffusion and diffraction. L=0 has a different signature with

#164287 - $15.00 USD Received 12 Mar 2012; revised 22 Apr 2012; accepted 24 Apr 2012; published 16 Oct 2012

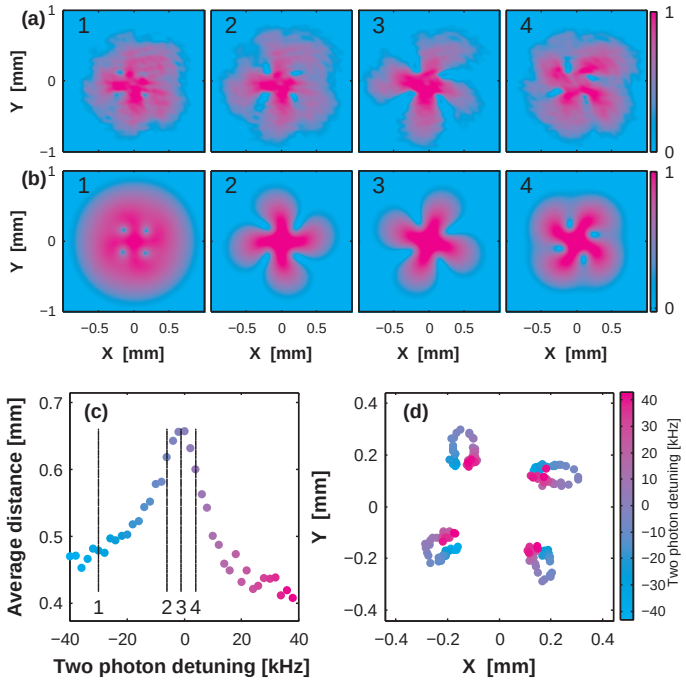

Fig. 4. Experimental results for the collective rotation of four m=+1 vortices with total angular momentum L=4. (a) Pictures for different frequencies with log scaled normalized intensity. The numbers relate to the vertical lines in (c). (b) Pictures of simulations for the same frequencies. (c) The average size of the array measured as the distance between two opposite vortices. (d) 2D plot of the vortex centers at different detunings. In this case, as with L=0, each vortex moves in a circular manner as the detuning is scanned, but here due to the fact that all the vortices rotate in the same direction, there is a global rotation of the entire array.

a global contraction (Fig. 3(c)) and no global rotation. This effect happens since each two adjacent vortices have inverse OAM thus leading to rotation in an opposite direction. Moreover, as the pattern with total OAM of L=0 contracts, the vortices start to join together leading to one large dark spot in the middle of the beam. Simulation shows that for strong enough interaction the global contraction for patterns may result in even a total annihilation of the vortices, in agreement with published free-space results of vortex dipoles [19].

As a quantitative measurement of the global rotation that arrays with L≠0 experience, we measure the angle of the connecting line between two vortices with respect to the x-axis. A total rotation span of more than 0.3 radians is visible (Fig. 5(a)).

The rotation has a dispersive signature, similar to the real part of the susceptibility, where it is possible to see an extra rotation in one side of the resonance and a contra free-space rotation on the other side. The EIT media in this case enables a manipulation of the effective optical path, thus allows us to change the optical pattern as if it was taken at different positions along the beam traveling axis. Actually, free space propagation like this would have taken about twice the Rayleigh length which is 1 meter in our case. In this view it is possible to think of the medium as a very high numerical aperture lens [12]. Moreover, contra free-space rotation is analogous to a backward movement of the beam from the origin. This effect is a signature of an index of refraction which is smaller than one. Figure 5(a) also demonstrates that positive or negative

#164287 - $15.00 USD Received 12 Mar 2012; revised 22 Apr 2012; accepted 24 Apr 2012; published 16 Oct 2012

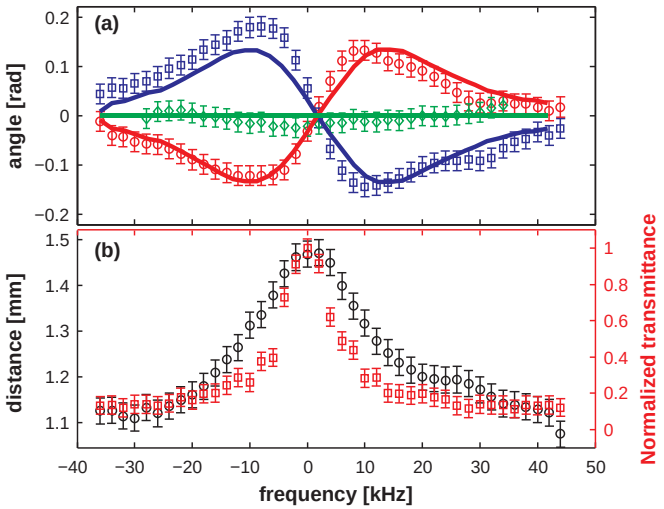

Fig. 5. (a) Rotation angle of two vortices. m=1(red circles), m=-1(blue squares), m=1 and m=-1 (green diamonds). Simulation results for these configurations are plotted by solid lines. (b) The distance between two m=+1 vortex centers (Black circles) and the EIT transmission (Red squares) as a function of the two photon detuning. Both curves follow the same trend.

total angular momentum creates an opposite rotation (blue squares and red circles curves), while zero OAM produces no rotation at all (green diamonds). Due to the imaginary part of the complex susceptibility an actual diffusion of the beam occurs. This effect was observed and measured before by Firstenberg et al. [20]. Here we show an easy way to measure it by looking at the average distance between vortices with the same optical angular momentum as depicted in Fig. 5(b). This increase in the distance between the vortices agrees well with the EIT line presented also in Fig. 5(b).

Larger arrays of vortices such as 3×3 and 4×4 were also created with similar effects as shown for the 2×2 array case. Due to the fact that the vortices cover a large part of the Gaussian beam, the EIT peak diminishes, thus leading to slightly less pronounced effects. As the dynamics of each vortex is affected by the local field in the point of the vortex, excluding the vortex itself, using a Gaussian field offers a way to manipulate even a single off-centered vortex alone [21]. Moreover, here we exploit the linear regime of the EIT media, but higher intensity will probe the nonlinear Kerr medium with extended rotation spans, not possible in the linear regime [16].

Vortex arrays can be stored in EIT media in a similar manner to previous experiments of storage of patterns using EIT [6, 11, 22]. We measure stored patterns of vortex arrays for different storage times. The stored patterns are similar to the patterns produced in the slow light regime apart from atomic diffusion effects that cause the dark center of the vortices to fill up as the storage time increases. This trend is in agreement with single vortex storage results presented by Pugatch et al. [11]. A typical measurement of such storage dynamics for two vortices with total L=0 can be seen in Fig. 6.

One advantage stored patterns have over slow light patterns is an enhanced purity of the measured vortex array state. The reason for this enhancement is the fact that only the EIT controlled light is stored. In contrast, in the slow light regime, various spectral contaminations can occur in the beam profile due to minor optical pumping effects and incoherent light.

#164287 - $15.00 USD Received 12 Mar 2012; revised 22 Apr 2012; accepted 24 Apr 2012; published 16 Oct 2012

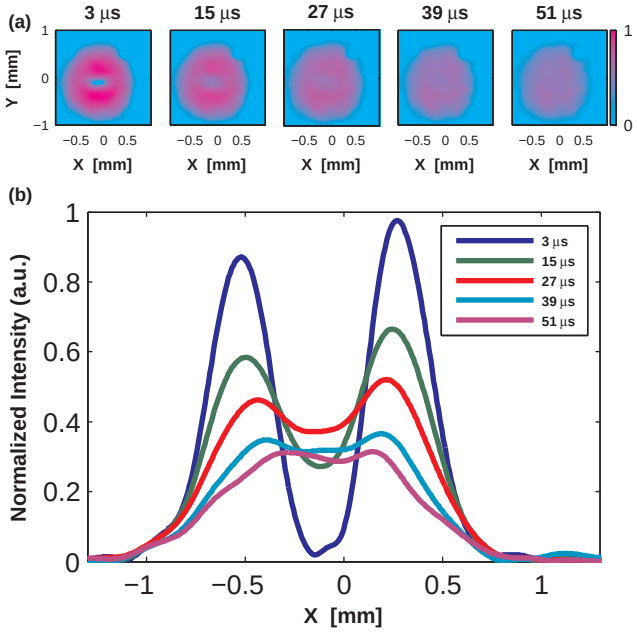

Fig. 6. Storage dynamics of two vortices with total L=0. The storage is done under the condition of zero two-photon detuning. (a) Pictures of the array for different storage times. (b) A cross section of the pictures in (a) along the axis connecting the two vortices. The vortices dark spot vanishes for long storage times.

4. Conclusion

We spectrally control the collective motion of optical vortex arrays by the use of EIT media. This control is done by changing the two photon detuning between the pump and probe beams. We describe how to use this method for various patterns of vortex arrays and explain the phenomenological differences between arrays with L=0 and L≠0, namely rotation and expansion of the array. This control may be used for fast and accurate displacement of optical vortices in applications such as optical wrenches and the transfer of optical angular momentum to particles [8]. The ability to detect small changes in the displacement of the vortices may also be used in magnetic sensing [23] and quantum measurements of multiphoton states with nontrivial spatial profiles.

Acknowledgments

We thank J. Howell and H. Eisenberg for fruitful discussions and comments. This work was supported by ISF grant No. 1248/10.

#164287 - $15.00 USD Received 12 Mar 2012; revised 22 Apr 2012; accepted 24 Apr 2012; published 16 Oct 2012